

Pulse Wave Imaging for Assessing Arterial Stiffness Change in A Mouse Model of Thoracic Aortic Dissection in Marfan Syndrome

Yuanyuan Wang¹, Chengwu Huang¹, Shuhong Ma², Qiong He¹, Feng Lan², and Jianwen Luo^{1*}

¹Department of Biomedical Engineering, School of Medicine, Tsinghua University, Beijing, China

²Beijing Laboratory for Cardiovascular Precision Medicine, Beijing Anzhen Hospital, Capital Medical University, Beijing, China

E-mail: luo_jianwen@tsinghua.edu.cn

Abstract—Marfan syndrome (MS) is a hereditary connective tissue disease characterized by the deflection of collagen complex and decrease of the connection between collagen and elastic fibers. Thoracic aortic dissection (TAD) is a common cause of death for patients with MS. In this study, we performed pulse wave imaging (PWI) in a β -aminopropionitrile (BAPN) induced, MS-relevant mouse model of TAD and measured the pulse wave velocities (PWVs) to assess the aortic stiffness related to the occurrence of TAD in MS. Three-week-old male mice were fed with regular diet (control group, $n = 6$) and diet with BAPN (BAPN group, $n = 10$) for 20 days, respectively. BAPN inhibits the cross-linking of collagen and elastin in systemic arteries, similar to TAD in MS patients, and could induce the occurrence of TAD in mice. PWI of the proximal abdominal aorta was performed every two days with a SonixMDP system and an L40-8 probe. Focused wave imaging with a reduced beam density was used to obtain a high frame rate of 980 Hz. The distension velocities of the aortic wall were estimated using speckle tracking and PWVs at the systolic foot (PWV_{sf}) and aortic notch (PWV_{dn}) were measured *in vivo*. Histologic examinations were performed on the thoracic aorta to confirm the presence of TAD. Statistical significance was assessed using two-tailed t tests. After 20 days of feeding, 8 mice from the BAPN group were found to have TAD in the histologic examinations. No significant differences in PWV_{sf} and PWV_{dn} were found between the control group ($n = 6$) and the TAD group ($n = 8$) before BAPN diet ($p = 0.60$ for PWV_{sf}, $p = 0.98$ for PWV_{dn}). In the last measurements after BAPN diet, PWV_{dn} from the TAD group was lower than that from the control group ($p < 0.05$), while no significant difference was observed in PWV_{sf} ($p = 0.48$). PWV_{dn} increased with the age of the mice for both the control and TAD groups, while the increment of PWV_{dn} between the last and first measurements was significantly lower in the TAD group ($p < 0.05$). Such difference was not found in PWV_{sf} ($p = 0.85$). These findings indicate that PWV_{dn} of the abdominal aorta can reflect the arterial stiffness change related to TAD and may be a promising index to monitor the aortic mechanical properties of MS.

Keywords—aortic stiffness, pulse wave velocity, thoracic aortic dissection.

I. INTRODUCTION

Marfan syndrome (MS) is a hereditary connective tissue disease characterized by the deflection of collagen complex

This study was supported in part by the National Natural Science Foundation of China (81561168023, 61871251 and 61801261) and the China Postdoctoral Science Foundation (2017M620802).

and decrease of the connection between collagen and elastic fibers [1]. These collagen-related changes can induce the dilation of the aortic wall to form an aneurysm or further induce the blood flow to break through the intima, tear the vessel wall and enter the middle layer to form a dissection. Once the aneurysm ruptures or the dissection is formed, the mortality rate is as high as 80% [2]. Therefore, the thoracic aortic aneurysm (TAA) rupture and thoracic aortic dissection (TAD) are very critical cardiovascular diseases and the major causes of death for patients with MS.

Once a TAA ruptures or TAD is identified, surgical treatment should be performed immediately. If the TAA has not ruptured, a trade-off between the surgical risk and rupture risk should be made when considering the treatment. In current clinical practice, the rupture risk is assessed based on the transverse diameter of the aneurysm [3]. However, studies have found that rupture can occur without a significantly increased diameter [4], while some aneurysms with large diameter are actually stable [5]. Therefore, a reliable method to assess the rupture risk is urgently needed in the decision-making of the clinical treatment.

Aortic stiffness is related to age and collagen properties, and has been indicated as an early predictor of cardiovascular mobility and all-cause mortality [6]. Pulse wave velocity (PWV) is widely used to characterize arterial stiffness and higher PWVs usually indicate higher arterial stiffness [7]. Clinically, PWV is calculated as the distance between two remote locations in the arterial tree divided by the time shift of the pulse waveforms from the two sites. However, the accuracy of this method suffers from measurement errors of distance and time-delay. Besides, PWVs at different locations along the arterial tree naturally vary [8]. Hence, non-invasive measurement of local PWV may better detect arterial stiffness change and improve the evaluation of cardiovascular diseases.

Pulse wave imaging (PWI) is a non-invasive method based on high-frame-rate ultrasound imaging for visualizing the propagation of pulse wave and measuring the local PWV along a vessel segment within the imaging field [9, 10]. This technique has been validated in mouse model of abdominal aortic aneurysm, and non-uniform propagation of pulse wave was found in the aneurysmal model [11]. Besides, PWV was found lower in unstable aneurysms than in the stable ones [12]. These findings demonstrate that PWI could potentially be used

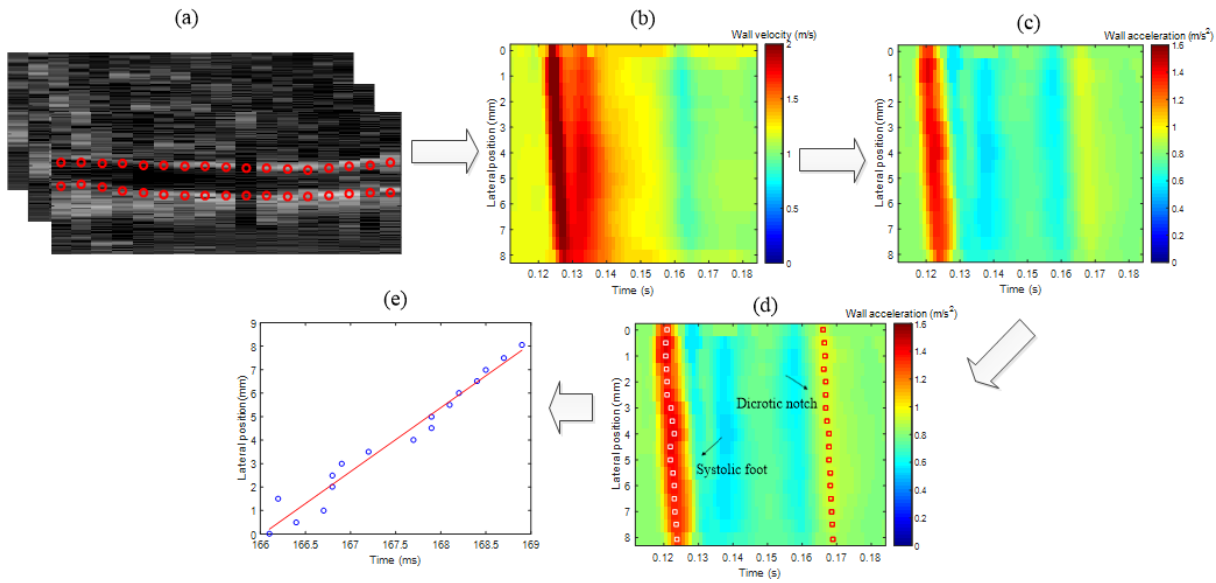


Fig. 1. The schematic overview of pulse wave velocity estimation procedure. (a) Ultrasound radiofrequency data acquisition in the long-axis view of abdominal aorta. The anterior and posterior walls were manually selected, as denoted by the red circles. (b) Spatio-temporal map of distension velocity obtained by estimating the aortic wall motion. (c) Spatio-temporal map of distension acceleration obtained by taking the temporal gradient of the corresponding distension velocity. (d) The exact locations of the systolic foot and dirotic notch were identified, as denoted by the white squares and red squares, respectively. (e) Linear regression between the characteristic time points of pulse waves determined by the dirotic notch and the lateral positions along the long axis of abdominal aorta. The PWV is equal to the reciprocal of the fitting line slope.

to assess the risk of abdominal aortic aneurysm rupture. Although the feasibility of PWV in human ascending aorta has been recently demonstrated [13], studies about the application of PWV in thoracic aneurysm and dissection are very limited. Therefore, in this study, we performed PWV in a β -aminopropionitrile (BAPN) induced model of TAD, which is close to the TAD in MS patients, and measured the PWVs to assess the aortic stiffness related to the occurrence of TAD in MS.

II. METHODS

A. Animal model

All procedures were approved by the Institutional Animal Care and Use Committee of Capital Medical University, Beijing, China. Sixteen three-week-old male C57B/L6 mice were obtained from HFK Bioscience Company (Beijing, China). Six mice were fed with regular diet for 20 days as the control group. The remaining ten mice received diet with a dose of 1g of BAPN per kilogram of the body mass per day for 20 days, recorded as the BAPN group. BAPN inhibits the cross-linking of collagen and elastin in systemic arteries, similar to TAD in MS patients, and could induce the occurrence of TAD in mice [14].

B. Data acquisition

For each mouse, PWV of the proximal abdominal aorta was performed every two days using a SonixMDP system (Analogic Corp., Peabody, MA, USA) with a linear array probe (L40-8/12). Three acquisitions (2 s each) were made to include about 20 cardiac cycles. Focused wave with 17 scan lines was transmitted to obtain a high frame rate of 980 Hz.

The transmit frequency of the probe was 10 MHz, and the sampling frequency was 40 MHz.

C. Data processing

All data was processed in MATLAB R2016a (The MathWorks, Natick, MA, USA). Figure 1 illustrates the procedure of PWV estimation. After acquiring the high-frame-rate ultrasound radiofrequency (RF) data, a normalized cross-correlation-based speckle tracking algorithm was used to estimate the inter-frame axial displacements [15]. The anterior and posterior aortic walls were manually detected on the B-mode images (indicated by the red circles in Fig. 1(a)). The axial velocities of the aortic wall were obtained as the corresponding inter-frame axial displacements multiplied by the frame rate (Fig. 1(b)). Distension velocity was then obtained by subtracting the velocities of the posterior wall from those of the anterior wall [16], which was further differentiated in the temporal domain to obtain the distension acceleration. The spatial-temporal map of the aortic wall distension accelerations in one cardiac cycle is displayed in Fig. 1(c). The systolic foot and the dirotic notch were extracted from the acceleration map by identifying the peaks of the corresponding acceleration waveforms before and after the systolic phase, as the feature points for determination of time delay, as denoted by the white squares and red squares in Fig. 1(d), respectively. Linear regression was performed between the characteristic time points and the corresponding beam locations, and PWV along the aortic segment was finally obtained as the reciprocal of the slope of the fitting line (Fig. 1(e)).

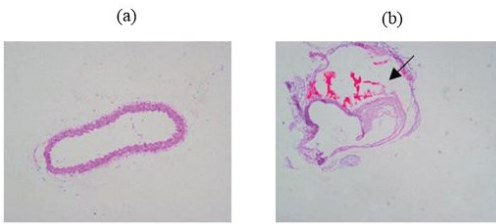


Fig. 2. Transverse histologic sections of thoracic aorta stained with H&E from (a) a mouse in the control group and (b) a TAD mouse in the BAPN group. The vessel laceration and blood in the pseudocavity (indicated by the arrow) confirms the occurrence of TAD.

D. Histopathology

At the end of the experiments (on day 20), all the remaining mice were executed and histopathology was performed on the aortas of all the sacrificed mice. During the histopathology, the thoracic aortas were fixed, embedded and sectioned with an interval of 7 μm . Several sections of each sample were stained with hematoxylin-eosin (H&E) and observed using a fluorescence microscope (ECIPSE80i/90i, Nikon, Tokyo, Japan).

III. RESULTS

Figure 2 shows transverse histologic sections obtained from the thoracic aortas of mice in the control group and the TAD group, respectively. The aortic wall laceration and blood in the pseudocavity (indicated by the arrow) observed in Fig. 2(b) confirm the occurrence of TAD.

In the BAPN group, 8 mice were found to have TAD, recorded as the TAD group, and no abnormalities were observed in the histologic examinations of the other two mice. PWVs at the systolic foot and dicrotic notch were compared in the abdominal aortas between the control group and the TAD group. All the TAD mice died around 16~20 days after taking BAPN diet and the last PWV measurements of these mice before death were compared with the last PWV measurements of the mice in the control group before the end of the experiments. Statistical significance was assessed using two-tailed t tests. As Fig. 3 shows, no significant differences in PWV_{sf} (control group: 2.89 ± 0.46 m/s, TAD group: 2.78 ± 0.33 m/s) and PWV_{dn} (control group: 2.68 ± 0.56 m/s, TAD group: 2.68 ± 0.29 m/s) were found between the control group and the TAD group before BAPN diet. In the last measurements after BAPN diet, PWV_{dn} was significantly lower in the TAD group (3.19 ± 0.36 m/s) than that in the control group (3.94 ± 0.66 m/s) ($p < 0.05$), while no significant difference was observed in PWV_{sf} (control group: 2.85 ± 0.64 m/s, TAD group: 2.66 ± 0.34 m/s) ($p > 0.05$). PWV_{dn} increased with the age of the mice for both the control group and TAD group, while the increment of PWV_{dn} between the last and first measurements was significantly lower in the TAD group (control group: 1.25 ± 0.79 m/s, TAD group: 0.51 ± 0.46) ($p < 0.05$). Such difference was not found in PWV_{sf} (control group: -0.04 ± 0.90 m/s, TAD group: -0.11 ± 0.62 m/s) ($p > 0.05$).

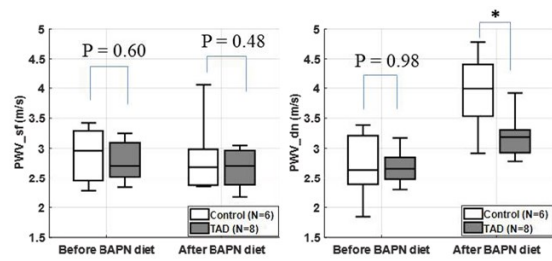


Fig. 3. Comparisons of PWV_{sf} and PWV_{dn} in the control group and TAD group. PWVs before BAPN diet were measured at the beginning of the experiment (on day 0). PWVs after BAPN diet were measured at the last presence of the mice. * indicates $p < 0.05$.

IV. DISCUSSION

Thoracic aortic aneurysm rupture and thoracic dissection could occur without warning and are the main causes of death for MS patients. The clinically used index, i.e., the maximum diameter of the aneurysm, is not reliable enough for assessing the TAA rupture risk. Aortic stiffness is known to be related to various cardiovascular diseases and may be a promising index for predicting the occurrence of TAD and TAA at early stage. Ultrasound imaging based PWI is a non-invasive method for quantitative characterization of local arterial stiffness by estimating the propagation velocity of pulse wave on an arterial wall segment. Therefore, in this study, PWI was performed on the abdominal aorta of a BAPN induced, MS-relevant mouse model of TAD, to assess the aortic stiffness related to the occurrence of TAD in MS.

As Figs. 3 and 4 show, before BAPN diet, no significant difference was found between the control group and the TAD group, for both PWV_{sf} and PWV_{dn}. But at around 20 days after BAPN diet, a decrease of PWV_{dn} was found in the TAD group, compared with the control group, indicating the aortic stiffness change in the TAD group. This finding is consistent with the mechanical changes reported in [17]. Such difference was not observed using PWV_{sf}, probably because PWV_{dn} has higher sensitivity in detecting aortic stiffness change than PWV_{sf} [16].

Because of the complex shape and small size of mouse thoracic aorta, the propagation distance of pulse wave can be easily misestimated in two-dimensional ultrasound imaging, inducing estimation error of PWVs. Besides, BAPN causes the deflection of collagen complex and decrease of the connection between collagen and elastic fibers in systemic arteries and may change the stiffness of both the abdominal aorta and thoracic aorta. Therefore, in this study, PWV on the abdominal aorta was measured to indirectly reflect the thoracic aortic stiffness related to the occurrence of TAD.

The mice in the BAPN group died of TAD at different days (at around 16 ~ 20 days) and for each mouse, the last measurements of the PWVs before death were used as the PWVs after BAPN diet, as displayed in Figs. 3 and 4. The effect of aging on the PWVs is not considered.

The sample size of the TAD mice in this study is limited, which may cause statistical errors. A larger sample size will be used in the future.

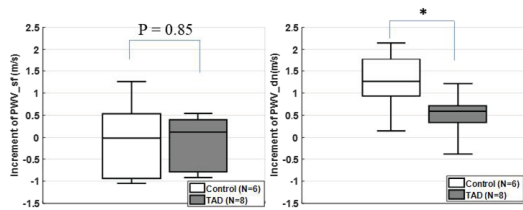


Fig. 4. Comparisons of the PWV_{sf} increments and PWV_{dn} increments in the control group and TAD group. PWV increment was obtained by subtracting the PWV measured at the last presence from the PWV measured at the beginning of the experiments. * indicates $p < 0.05$.

V. CONCLUSION

In this study, we developed a BAPN induced mouse model of TAD, similar to the TAD in Marfan syndrome patients. PWVs of the abdominal aortas were measured to indirectly assess the thoracic aortic stiffness change related to the occurrence of TAD. PWVs at the systolic foot and diastolic notch were compared in the abdominal aortas between mice from the control group and mice identified with TAD. At the beginning of the experiments, no significant differences in PWV_{sf} and PWV_{dn} were found between the control group and the TAD group. At the end of the experiments, the PWV_{dn} from the TAD group was significantly lower than that from the control group, while no difference was found between these two groups using PWV_{sf}. The increment of PWV_{dn} from the TAD group is significantly lower than that from the control group. Such difference was not found in PWV_{sf}. These findings demonstrate that local PWV (more specifically, PWV_{dn}) may be used to characterize the change in aortic wall stiffness related to TAD and could be potentially used as an index for assessing the risk of TAD and TAA rupture in MS patients.

REFERENCES

- [1] H. C. Dietz, G. R. Cutting, R. E. Pyeritz, C. L. Maslen, L. Y. Sakai, G. M. Corson, *et al.*, "Marfan syndrome caused by a recurrent de novo missense mutation in the fibrillin gene," *Nature*, vol. 352, pp. 337-339, 1991.
- [2] B. S. Brooke, J. P. Habashi, D. P. Judge, N. Patel, B. Loeys, and H. C. Dietz III, "Angiotensin II blockade and aortic-root dilation in Marfan's syndrome," *New England Journal of Medicine*, vol. 358, pp. 2787-2795, 2008.
- [3] J. A. Elefteriades and E. A. Farkas, "Thoracic aortic aneurysm: clinically pertinent controversies and uncertainties," *Journal of the American College of Cardiology*, vol. 55, pp. 841-857, 2010.
- [4] J. F. Rodríguez, R. Cristina, D. Manuel, and G. A. Holzapfel, "Mechanical stresses in abdominal aortic aneurysms: influence of diameter, asymmetry, and material anisotropy," *Journal of Biomechanical Engineering*, vol. 130, p. 021023, 2008.
- [5] P. W. Stather, N. Dattani, M. J. Bown, J. J. Earnshaw, and T. A. Lees, "International variations in AAA screening," *European Journal of Vascular & Endovascular Surgery*, vol. 45, pp. 231-234, 2013.
- [6] H. Sato, J. Hayashi, K. Harashima, H. Shimazu, and K. Kitamoto, "A population-based study of arterial stiffness index in relation to cardiovascular risk factors," *Journal of Atherosclerosis and Thrombosis*, vol. 12, pp. 175-180, 2005.
- [7] D. Justine Ina and A. D. Struthers, "Pulse wave analysis and pulse wave velocity: a critical review of their strengths and weaknesses," *Journal of Hypertension*, vol. 21, pp. 463-472, 2003.
- [8] M. C. Whitlock and W. G. Hundley, "Noninvasive imaging of flow and vascular function in disease of the aorta," *Jacc Cardiovascular Imaging*, vol. 8, pp. 1094-1106, 2015.
- [9] J. Vappou, J. Luo, and E. E. Konofagou, "Pulse wave imaging for noninvasive and quantitative measurement of arterial stiffness in vivo," *American Journal of Hypertension*, vol. 23, pp. 393-398, 2010.
- [10] J. Luo, R. X. Li, and E. E. Konofagou, "Pulse wave imaging of the human carotid artery: an in vivo feasibility study," *IEEE Transactions on Ultrasonics, Ferroelectrics, and Frequency Control*, vol. 59, pp. 174-181, 2012.
- [11] J. Luo, K. Fujikura, L. S. Tyrie, M. D. Tilson, and E. E. Konofagou, "Pulse wave imaging of normal and aneurysmal abdominal aortas in vivo," *IEEE Transactions on Medical Imaging*, vol. 28, pp. 477-486, 2008.
- [12] S. D. Nandlall and E. E. Konofagou, "Assessing the stability of aortic aneurysms with pulse wave imaging," *Radiology*, vol. 281, pp. 772-781, 2016.
- [13] C. Huang, D. Guo, F. Lan, H. Zhang, and J. Luo, "Noninvasive measurement of regional pulse wave velocity in human ascending aorta with ultrasound imaging: an in-vivo feasibility study," *Journal of Hypertension*, vol. 34, pp. 2026-2037, 2016.
- [14] E. Martínez-Martínez, C. Rodríguez, M. Galán, M. Miana, R. Jurado-López, M. Luaces, *et al.*, "The lysyl oxidase inhibitor (β -aminopropionitrile) reduces leptin profibrotic effects and ameliorates cardiovascular remodeling in diet-induced obesity in rats," *Journal of Molecular & Cellular Cardiology*, vol. 92, pp. 96-104, 2016.
- [15] J. Luo and E. E. Konofagou, "A fast normalized cross-correlation calculation method for motion estimation," *IEEE Transactions on Ultrasonics, Ferroelectrics, and Frequency Control*, vol. 57, pp. 1347-1357, 2010.
- [16] C. Huang, Y. Su, H. Zhang, L. X. Qian, and J. Luo, "Comparison of different pulse waveforms for local pulse wave velocity measurement in healthy and hypertensive common carotid arteries in vivo," *Ultrasound in Medicine & Biology*, vol. 42, pp. 1111-1123, 2016.
- [17] L. E. Jackson, B. Faris, B. M. Martin, H. V. Jones, C. B. Rich, J. A. Foster, *et al.*, "The effect of β -aminopropionitrile on elastin gene expression in smooth muscle cell cultures," *Biochemical and Biophysical Research Communications*, vol. 179, pp. 939-944, 1991.